



# Analyzing the variation of the precipitation of coastal areas of eastern China and its association with sea surface temperature (SST) of other seas

Chenxu Ji<sup>a</sup>, Yuanzhi Zhang<sup>a,b,\*</sup>, Qiuming Cheng<sup>c,\*\*</sup>, Yu Li<sup>d</sup>, Tingchen Jiang<sup>e</sup>, X. San Liang<sup>a</sup>

<sup>a</sup> Nanjing University of Information Science and Technology, School of Marine Sciences, Nanjing 210044, China

<sup>b</sup> Chinese University of Hong Kong, Center for Housing Innovations, Shatin, Hong Kong

<sup>c</sup> China University of Geosciences, State Key Laboratory for Geological Processes and Mineral Resources, Beijing 100083, China

<sup>d</sup> Beijing University of Technology, Faculty of Information Science, Beijing 100124, China

<sup>e</sup> School of Geomatics and Marine Information, HuaiHai Institute of Technology, Lianyungang 222005, China

## ARTICLE INFO

### Keywords:

Precipitation  
Sea Surface Temperature  
Coastal areas of the Eastern China  
Seasonal variation  
Inter-annual variation

## ABSTRACT

In this paper, we analyzed the effect of SST on the precipitation of coastal areas of the eastern China. The relationship between the precipitation and SST of different seasons based on CMDC's monthly precipitation data and NOAA's SST data from 1979 to 2016 was calculated. Analysis on the links between precipitation and SST has shown a significant correlation in winter and spring, with three positive strong oceanic signals and two negatively correlated sea areas. Meanwhile, the precipitation and SST of highly correlated regions have increased during the past 38 years. Considering the seasonal variation, precipitation presents upward trend in summer and winter with appreciable seasonal variations. For one of the highly related areas, such as the East China Sea (ECS) and the north of Philippine Sea (PS), the SST there has been increased in all four seasons. Spectral analysis also shows that the precipitation and the MEI have the same cycles about 3–5 years. Moreover, lead-lag analysis between precipitation time-series and three climate indexes (Niño 1 + 2 SST index, Niño 3 SST index and SIOD SST index) were applied. The results show that when the SSTs lead 2 to 4 months, they are highly related to the precipitation in the coastal areas of the eastern China.

## 1. Introduction

Dominated by the East Asian monsoon, an energetic component of the global climate system, the coastal areas of eastern China are featured by high temperature, moist and rainy in summer and low temperature, dry and rainless in winter. And the development of the coastal areas of the eastern China is quite vulnerable to the variability of the climate in this region, especially the precipitation (Tao, 1987; Yu and Zhou, 2007; Zhu et al., 2011; Cai et al., 2017; Zhang and Ge, 2013). Being largely affected by the monsoonal circulation and external forcing, precipitation over the coastal areas of the eastern China has distinct seasonal characteristics. The precipitation presents an upward (downward) trend in summer (winter) over there. More than this, the precipitation has inter-annual variabilities with frequent floods and droughts (Webster et al., 1998; Yang and Lau, 2004; Ding et al., 2008; Ji et al., 2018a).

According to the previous studies, in the late 1970s, the precipitation became more plentiful in the Yangtze River valley, and reduced in

the north of China. However, some researchers claimed that the precipitation pattern in the East China had changed since 1999, of which the rainfall decreased in the Yangtze River region but there had been a tendency for enhanced precipitation in the Huang-Huai River region (Ding et al., 2009; Li and Leung, 2013; Zhu et al., 2011; Ji et al., 2018b). Moreover, because of the continental and oceanic processes and global warming, the precipitation over the Southeast China is influenced by the large-scale atmospheric circulation (Zhang et al., 2015; Li et al., 2010a, 2010b).

It is claimed that many factors could affect the precipitation over the eastern China, and some of them have been demonstrated to be the major determinants, such as sea surface temperature (SST), Tibetan Plateau heating, Tibetan Plateau snow cover and polar ice coverage (Liu et al. (2014a, 2014b); Yang and Lau, 2004; Zhu et al., 2015; Ji et al., 2018a). In addition, El Niño–Southern Oscillation (ENSO), Siberian High and East Asian trough would also influence the inter-annual variability of precipitation there. Among all the factors, SST has been identified to dominate the decadal variability of precipitation in

\* Corresponding author at: Nanjing University of Information Science and Technology, School of Marine Sciences, Nanjing 210044, China.

\*\* Corresponding author.

E-mail addresses: [yuanzhizhang@cuhk.edu.hk](mailto:yuanzhizhang@cuhk.edu.hk) (Y. Zhang), [qiuming.cheng@iugs.org](mailto:qiuming.cheng@iugs.org) (Q. Cheng).

the eastern China (Li et al., 2010a, 2010b; Zhou et al., 2010; Zhou and Wu, 2010). It is of great importance to predict the rainfall by identifying the relationship between SST and precipitation (Kumar et al., 2013).

Due to the variations of surface evaporation, low-level moisture convergence and thermal convection caused by SST anomalies, the rainfall would be abnormal in the coastal areas. And this positive SST-precipitation correlation is a typical pattern in some areas (Wu and Kirtman, 2007).

The study of the influence of ENSO on precipitation can date back to the early 1920s (Walker, 1925). Since 1980's, there have been more and more works focusing on detecting the relationship between ENSO and precipitation (Rasmusson and Wallace, 1983; Shukla and Paolino, 1983). Because of the transform of ENSO pattern (shift from conventional ENSO to ENSO-Modoki), the rainfall over the South China and many other areas has changed (Feng and Li, 2011; Zhang et al., 2011; Ji et al., 2018b). Yang and Lau (2004) had demonstrated that it was the warming trend of the ENSO-like mode that contributes to the increase of spring precipitation over the southeastern China and decrease over the northern China. Meanwhile, the interdecadal variations of summer monsoon rainfall over the South China are found to be associated with the ENSO (Chan and Zhou, 2005).

Teleconnections between ENSO and precipitation over the eastern China and Yangtze catchments also have been analyzed before. According to the previous researches, ENSO shows a close relation with the seasonal precipitation variability over there (Xiao et al., 2015; Tong et al., 2006; Yang and Lau, 2004). What's more, flood and drought events were found to be closely related with El Niño and La Niña (Ouyang et al., 2014; Tong et al., 2006). About the mechanism of this phenomenon, many works have been done. One of the researchers put up a mechanism named Pacific–East Asia teleconnection to explain how ENSO affects precipitation, which highlights the significance of air–sea interaction over the Philippine Sea (Wang et al., 2000). Another explanation emphasizes the strength of the subtropical high in the western Pacific region (Tong et al., 2006).

It has been documented in the earlier studies that positive Indian Ocean Dipole (IOD) events would generate a Rossby wave train and induce the precipitation anomalies in the East China (Guan and Yamagata, 2003; Xie et al., 2009). What's more, the positive IOD event would increase the rainfall in different regions of the Yangtze River basin among different seasons (Xiao et al., 2015; Yuan et al., 2008). Xu et al. (2013) found a close relationship between Subtropical Indian Ocean Dipole (SIOD) and rainfall over China. Because of the anticyclonic atmosphere anomalies over the South China Sea and Philippine Islands, SIOD would cause anomalous precipitation (Xu et al., 2013).

Summing up previous studies, much work had been done to detect the relationship between precipitation and SST, seldom did they consider SSTs' effects on the precipitation of the coastal areas of eastern China. Not only that, the studies involved the seasonal and inter-annual diversity of precipitation, while SST and their correlation are little reported.

The objectives of this paper are to document the variability of the precipitation over coastal areas of the eastern China and its links to the SSTs in different seasons and different oceanic regions of other seas. Furthermore, we would examine the lead-lag relationship between the precipitation and several climate time-series (e.g. Niño 1 + 2 SST index, Niño 3 SST index, MEI and SIOD SST index).

## 2. Data and methods

### 2.1. Data

#### 2.1.1. NOAA data

Monthly mean SST data from 1979 to 2016 are derived from National Oceanic and Atmospheric Administration (NOAA) Extended Reconstructed Sea Surface Temperature (SST) V5 dataset ([https://](https://www.esrl.noaa.gov/psd/data/gridded/data.noaa.ersst.v5.html)

[www.esrl.noaa.gov/psd/data/gridded/data.noaa.ersst.v5.html](https://www.esrl.noaa.gov/psd/data/gridded/data.noaa.ersst.v5.html)), with a horizontal resolution of  $2.0^\circ \times 2.0^\circ$  global grid ( $180 \times 89$ ).

#### 2.1.2. CMDC version 2.0 combined precipitation data set

Monthly precipitation dataset is provided by China Meteorological Data Service Center (CMDC) from 1979 to 2016. It combines ground observations data and model precipitation data into  $0.5^\circ \times 0.5^\circ$  horizontal resolutions (<http://data.cma.cn/site/showSubject/id/46.html>). In this paper, monthly precipitation data of eastern China ( $115^\circ \sim 122^\circ \text{E}$  and  $22^\circ \sim 38^\circ \text{N}$ ) is processed into regional mean value.

#### 2.1.3. Climate time-series

Monthly Niño 1 + 2 SST index and Niño 3 SST index from 1979 to 2016 are derived from NOAA's Earth System Research Laboratory (<https://www.esrl.noaa.gov/psd/enso/data.html>).

The SIOD index is computed from SST anomaly difference between western ( $55^\circ\text{--}65^\circ\text{E}$ ,  $37^\circ\text{--}27^\circ\text{S}$ ) and eastern ( $90^\circ\text{--}100^\circ\text{E}$ ,  $28^\circ\text{--}18^\circ\text{S}$ ) Indian Ocean (Behera and Yamagata, 2001). We firstly calculated the monthly mean SST of the two areas separately and then compared the difference between them using the SIOD index.

## 2.2. Methods

### 2.2.1. Correlation analysis

The Pearson correlation coefficient (PCC) is a measure of detecting the degree of association between two variables as  $X$  and  $Y$  (Pearson, 1895). The formula is:

$$r = \frac{1}{n-1} \sum_{i=1}^n \left( \frac{X_i - \bar{X}}{S_x} \right) \left( \frac{Y_i - \bar{Y}}{S_y} \right) \quad (1)$$

where  $n$  is the size of variable  $X$  and  $Y$ ,  $S_x$  and  $S_y$  are the standard deviation of  $X$  and  $Y$ , and  $\bar{X}$  and  $\bar{Y}$  are the mean value of  $X$  and  $Y$ .

In this study we used the PCC to discuss the relationship between the precipitation and SST of each four seasons during the period of 1979 to 2016, and figured out whether the SST would affect the precipitation above the eastern China.

### 2.2.2. Mann–Kendall test

The Mann–Kendall (MK) trend test is used to statistically assess if there is a monotonic upward or downward trend of the variable of interest over time (Mann, 1945; Kendall, 1975). It uses the parameter  $Z_c$  (Yue and Wang, 2004) to measure whether the trend is significant. When  $|Z_c|$  is greater or equal to 1.28, 1.64, and 2.32, respectively, it means that they respectively pass the test under 90%, 95% and 99% significance (Yue and Wang, 2004).

Here the M-K test is applied to the seasonal and yearly mean precipitation and SST dataset, to check whether their trends are significant during our study period.

### 2.2.3. Standard score

In statistics, a standard score refers to the standard deviation of the values of observation points or data points higher than the average values of observed or measured. It is calculated by (Erwin, 1979):

$$K_i = \frac{X_i - \bar{X}}{S} \quad i = 1, 2, 3, \dots, n \quad (2)$$

where  $X_i$  is the value of sample,  $\bar{X}$  is the mean, and  $S$  represents the standard deviation. A positive standard score represents that the observation value is above the average value, while negative standard scores means the values below the average. Here, we take  $\pm 1$  as the threshold to measure whether the value is abnormal.

We processed the precipitation of eastern coastal areas of China, the Niño3 SST index and the SIOD index into the standard index to find out their variation tendency and then discussed the relationship among them.

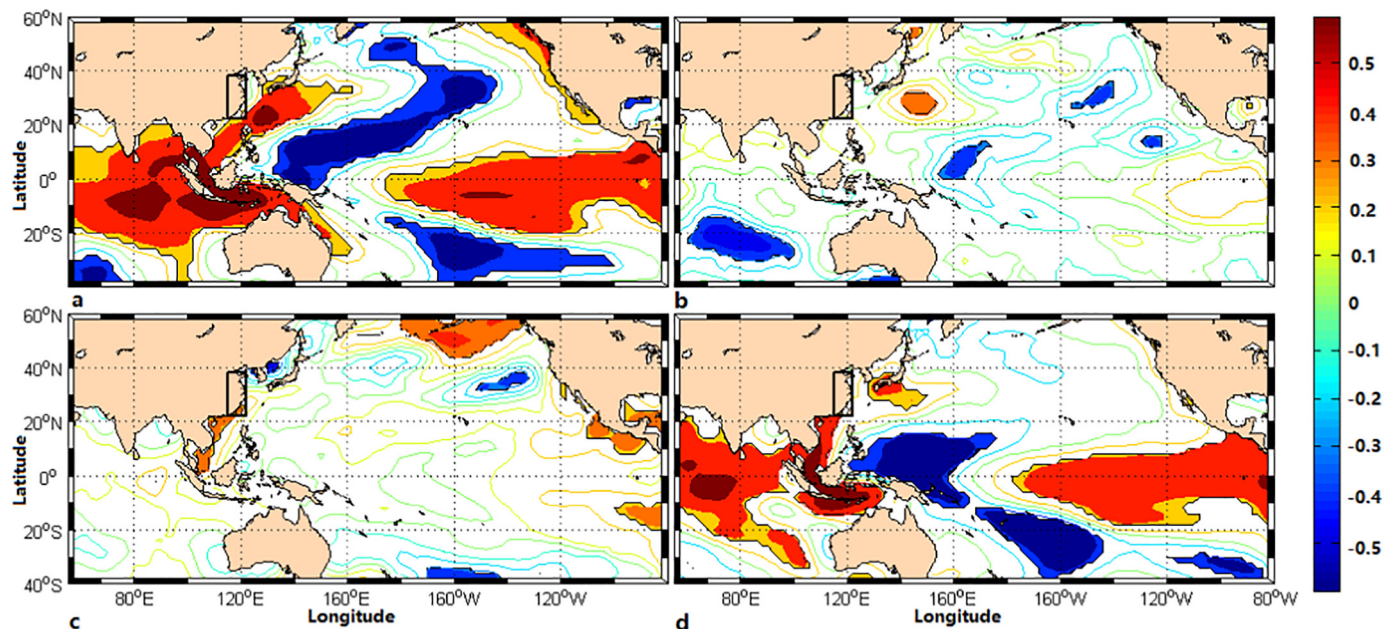


**Fig. 1.** Correlation between the precipitation and SST of 4 seasons during the period of 1979 to 2016 (a: spring; b: summer; c: autumn; d: winter; the areas passing 95% significance test are colored; before the correlation analysis on the SSTs and precipitation time series, the data were de-trended).

**Table 1**

The correlation coefficient of mainly correlated area of four seasons.

Area season	ECS&PS	EEP	SIO
Spring(a)	0.4076	0.4757	0.5562
Summer(b)	0.1775	0.1251	-0.1033
Autumn(c)	0.0302	0.1381	0.0983
Winter(d)	0.3310	0.5073	0.4820

#### 2.2.4. Spectral analysis

In order to detect the cyclical patterns of the precipitation and SST, the spectral analysis is applied to the data, which can decompose a complex time series into several sinusoidal functions (Korn et al., 1998; Pelletier, 1998; Ghil et al., 2002). Here we used the single Fourier analysis to discuss the periodicity in the precipitation and SST. Before analysis, the data were de-trended.

### 3. Result and discussion

#### 3.1. Correlation between the precipitation of coastal areas of eastern China and SST

In the coastal areas of the eastern China (the black rectangular area in Fig. 1; 115°–122°E and 22°–38°N), we calculated the seasonal precipitation. Using eq. 1, we got the distribution of correlation between the precipitation and SST of four seasons during the period of 1979 to 2016 (Fig. 1). Colored areas of the figure represent high correlation between precipitation and SST, with the correlation coefficients passing the *t*-test, at a confidence level of 95%.

Three main correlated areas can be seen in Fig. 1.a. They are located in the East China Sea (ECS) and the north of Philippine Sea (PS) (130°–150°E and 25°–35°N), Eastern Equatorial Pacific (EEP) (150°–90°W and 5°S–5°N), and subtropical Indian Ocean (SIO) (60°–90°E and 15°S–0°), respectively. However, the acreage of correlated areas varies from spring (Fig. 1.a) to winter (Fig. 1.d). The distribution is wider in winter and spring. But they gradually turn to small in summer and autumn. Meanwhile, in spring, summer and winter, there is a negatively correlated area in the Western Equatorial Pacific, which is near to the Western Pacific Warm Pool (WPWP). The WPWP

occupies the largest expanse of the Earth's surface of the highest water temperatures. Some scholars pointed out that there is a significant correlation between the precipitation over the eastern China and the West Pacific Warm Pool over the summer (Mao-qi et al., 2004). Also, in the south-western Indian Ocean, a negatively correlated area occurs in spring and summer. The results are consistent with the previous studies, in which they analyzed the relationship between precipitation and SST, and came to the conclusion that it was significantly positively correlated in the tropical Indian Ocean and Pacific Ocean, negatively correlated over the western Pacific, eastern SCS, and the Bay of Bengal (Wang et al., 2005; Wu et al., 2009; Lu and Lu, 2014).

Table 1 gives the correlation coefficient for each mainly positively correlated area of four seasons. We can see that they have higher values in spring and winter. It means that the precipitation of coastal areas of the eastern China is highly related to the winter and spring SST, especially in the SIO of spring-time, of which the coefficient reaches 0.5562. In comparison, the coefficient is lower in summer and autumn, and it turns to be negatively correlated in the SIO of summer-time.

#### 3.2. Seasonal and inter-annual variation of the precipitation of coastal areas of eastern China and SST in correlated areas

##### 3.2.1. Seasonal and inter-annual variation of the precipitation

To further study the correlation between SST and precipitation of coastal areas of eastern China, the variations of them are analyzed. Fig. 2 shows the monthly average precipitation of coastal areas of the eastern China, in which the value slightly rises from winter (December, January and February) to spring (March, April and May) and reaches its maximum in summer (June, July and August). Then, it drops in autumn (September, October and November). The summer precipitation is nearly 4 times that in winter.

Fig. 3 shows the variation of precipitation in coastal areas of the eastern China of four seasons. There is an upward trend in summer and winter during the period of 1979–2016 as revealed by previous studies (e.g. Yang and Lau, 2004), and the upward trend in summer is significant (passed the M-K test at a confidence level of 95%, with the value  $Z_c = 2.02$ ). The precipitation in spring and autumn had experienced a slight drop during the past 38 years. But the downward trend was not significant.

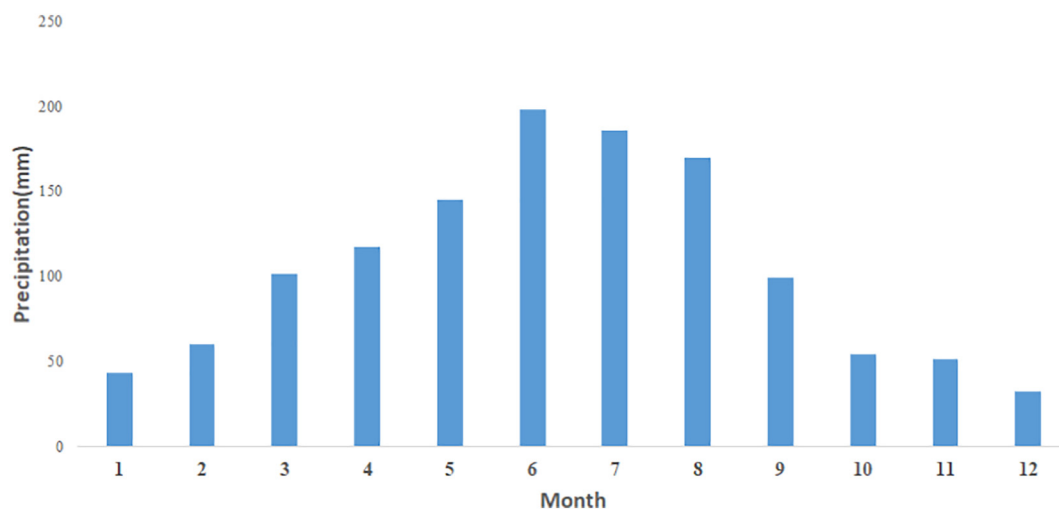


Fig. 2. Monthly average precipitation of coastal areas of eastern China; (unit: mm).

3.2.2. Seasonal and inter-annual variation of SST

Here we take one of the positively correlated areas (East China Sea (ECS) and the north of Philippine Sea (PS)) in Fig. 1 as example to calculate the monthly average SST there. Fig. 4 shows the SST for each month in the selected area. The temperature consistently rises from May to August, but it subsequently drops from September to February. The average temperature there is 23.4 °C.

The inter-annual SST variation of the four seasons in this area is presented in Fig. 5. All the four seasons' SSTs have been rising during the past 38 years, and the upward trends of SSTs in summer, autumn and winter have passed the M-K test at a confidence level of 95%. The average value of each four seasons is computed. The results show that the summer has the highest value of 26.5 °C, but the SSTs in winter and spring are low, which is similar to the previous study of Gong and Wong (2018).

3.2.3. Seasonal and inter-annual variation of the correlation between the precipitation and SST

The variation of precipitation in coastal areas of the eastern China is greatly affected by the East Asian monsoon, with significant inter-annual and inter-decadal variabilities (Ding et al., 2008). Fig. 6 depicts the inter-annual variation of precipitation and the precipitation anomaly. Although the precipitation shows a significant downward trend in the periods 1983–1986, 1998–2004 and 2005–2009, it is fluctuating upward during the past 38 years on the whole. This is the same as the result of Zhu et al. (2011), in which the researchers claimed that the precipitation pattern in East China had changed appreciably since 1999.

Especially, in the past four years, the increase in precipitation is very significant. Moreover, we can see the obvious inter-annual variation from the precipitation anomaly (the bar graph in Fig.6).

Focusing on the three downward periods, we found that they all

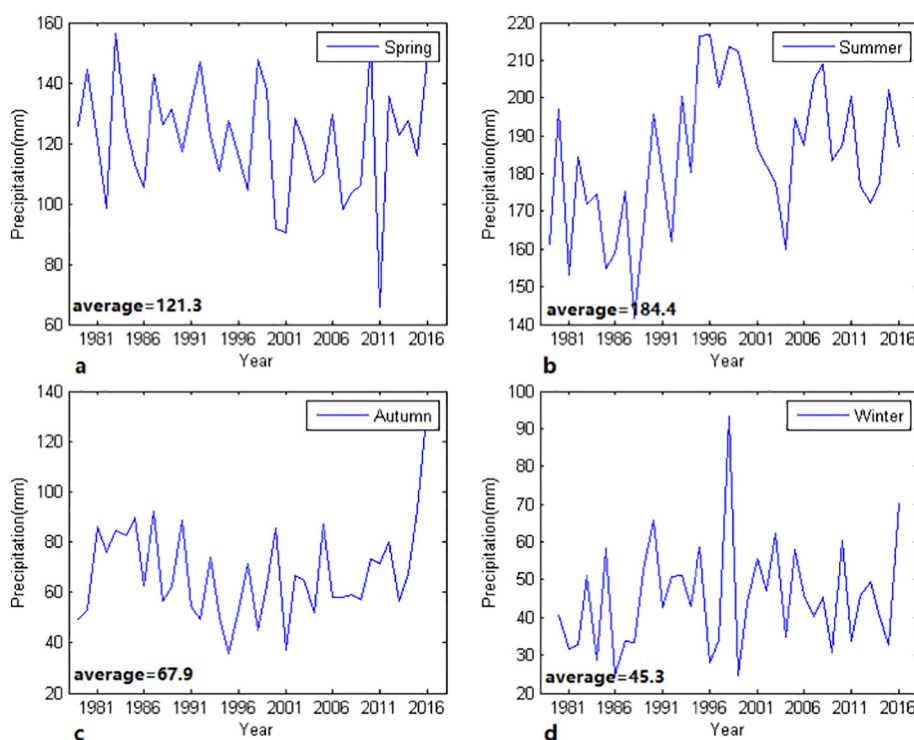


Fig. 3. The variation of precipitation of four seasons in coastal areas of eastern China (a: spring; b: summer; c: autumn; d: winter; unit: mm).

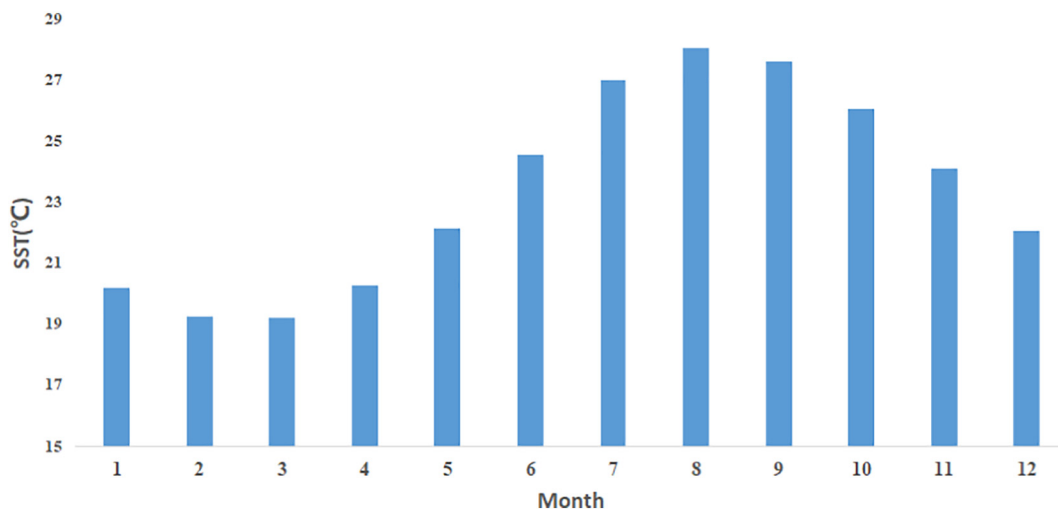


Fig. 4. Monthly average SST of East China Sea (ECS) & the north of Philippine Sea (PS) (unit: °C).

came after the El Niño events. They occurred in 1982–1983, 1997–1998 and 2004–2005 with the first two events among the strongest on record (Center, 2015).

Fig.7 indicates the power spectra for the precipitation over the eastern China (Fig.7 a) and the multivariate ENSO Index (MEI) (Fig.7 b) during the period 1979–2016. We can see from the figure that the three main cycles of the precipitation are 3.17, 2.24 and 6.33 years. For the MEI they are 5.43, 3.8 and 12.67 years respectively. These two sets of results show that the time series of precipitation over the eastern China and the MEI have the similar cycles about 3 and 5 years, in which the correlation is obvious between the precipitation and ENSO events.

For the selected correlated areas in fig. 1 (East China Sea (ECS) & the north of Philippine Sea (PS); Eastern Equatorial Pacific (EEP); and Subtropical Indian Ocean (SIO)), the annual average SSTs are calculated respectively (Fig.8). All of the three SSTs have increased during the period of 1979–2016. The ECS & PS's SST rises from 22.7 °C to about

24.2 °C, and the EEP's SST rises from 25.7 °C to 26.6 °C. It increases from 27.6 °C to 28.5 °C in SIO, in which, the upward trends of SSTs in ECS & north of PS and SIOD pass the M-K test at a confidence level of 95%.

The inter-annual variation of precipitation (Fig.6) and the SSTs (Fig.8) shows a similar trend. In addition, the location of EEP has almost overlap with the area of Niño 1 + 2 (90°~80°W and 10°S~0°) and Niño 3 (150°~90°W and 5°S~5°N), two of the Niño regions. Another related area SIO in Fig. 1 has a high overlap level with the position of Subtropical Indian Ocean Dipole (SIOD), which is characterized by the oscillation of SST in the southwest Indian Ocean. The water is warmer in the south-western part of the Indian Ocean, such as south of Madagascar, and then turns to be colder than the eastern part of the Indian Ocean in positive SIOD phase (Behera and Yamagata, 2001). In a boreal winter, the positive (negative) SIOD events are always accompanied by the weak (strong) Indian summer monsoons, which would cause a weakening (strengthening) of the monsoon circulation system in a

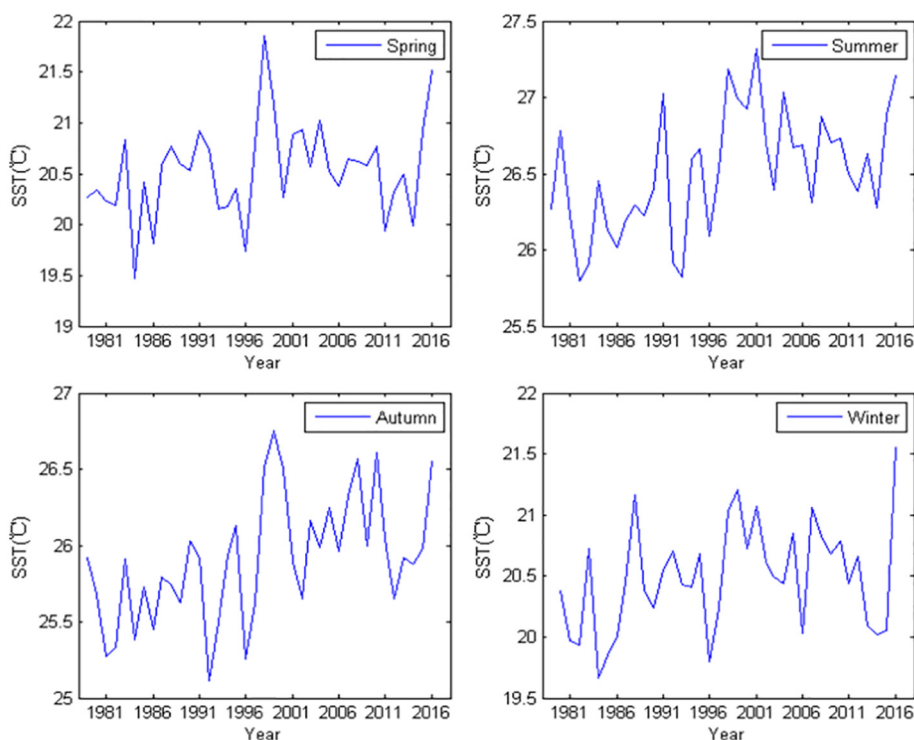


Fig. 5. The variation of SST of East China Sea (ECS) & the north of Philippine Sea (PS) (a: spring; b: summer; c: autumn; d: winter; unit: °C).

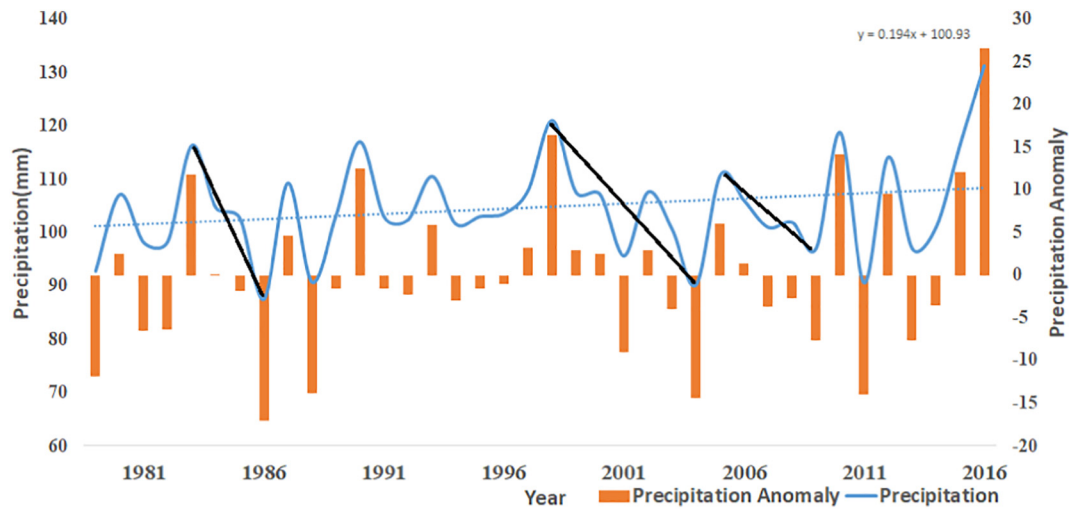


Fig. 6. The inter-annual variation of precipitation in coastal areas of eastern China (blue line, unit: mm); and precipitation anomaly (red bar graph).

boreal summer. It would also affect the precipitation in many regions (Privé and Plumb, 2007; Qiuming, 2006; Terray et al., 2003).

To further study the relationship between SST and precipitation in coastal areas of eastern China. The standard indices of precipitation, Niño 1 + 2 SST, Niño 3 SST, and SIOD SST are shown in Fig. 9. It is clear that all of the three standard indexes have the similar fluctuation and cycle. We noted that there is a lead-lag relationship between the precipitation and the three climate time-series index. The antecedent SST is significantly correlated to the subsequent precipitation.

Then we investigated lead-lag relationships between precipitation in coastal areas of eastern China and each three climate index using lagged correlations. Table 2 is the correlation coefficients between the standard index of precipitation and each climate index, and all the values passed the significance testing at a level of 95%. Table 2 implies that when Niño 1 + 2 index leads rainfall by 3-month, the precipitation and SST indices are significantly positively correlated with the coefficient about 0.7835. This result is similar to those of when the Niño 3 index leads precipitation by a 2- or 3-month period, and the coefficients reach 0.6768 and 0.6409, respectively. For the SIOD index, precipitation leads it a 4-month period to reach the highest correlation coefficient about 0.5609. This result is very close to some earlier studies (e.g. Wang et al., 2005).

#### 4. Conclusions

In this study, using the CMDC precipitation data and NOAA's SST data, we analyze the variability of the precipitation in coastal areas of eastern China and its links to global SSTs. This article starts from the assumption that the eastern China's precipitation and its variability might be associated with the SST. Firstly, we applied correlation analysis to the SST and precipitation in different seasons. The results vary from season to season. They are more significant in winter and spring, and three major areas are found to be highly correlated to the precipitation. They are the East China Sea (ECS) and the north of Philippine Sea (PS), Eastern Equatorial Pacific (EEP), and subtropical Indian Ocean (SIO), respectively. Also, there are two main negative correlation areas (located in WPWP and the South Pacific).

The seasonal and inter-annual variation of precipitation and SST are calculated respectively. The precipitation is heavy in spring and summer, and it's almost 2 or 3 times that in autumn and winter. Considering the inter-annual variation of the precipitation, it is consistently rising in summer and winter. But the precipitation in spring and autumn had experienced slightly drop during the period of 1979–2016. However, it is fluctuating upward during the past 38 years on the whole, especially in the past 4 years, the upward is very significant. For the SST in three correlated areas, all of them have been increasing during this period, about 1.1 °C on average. Focus on the ECS

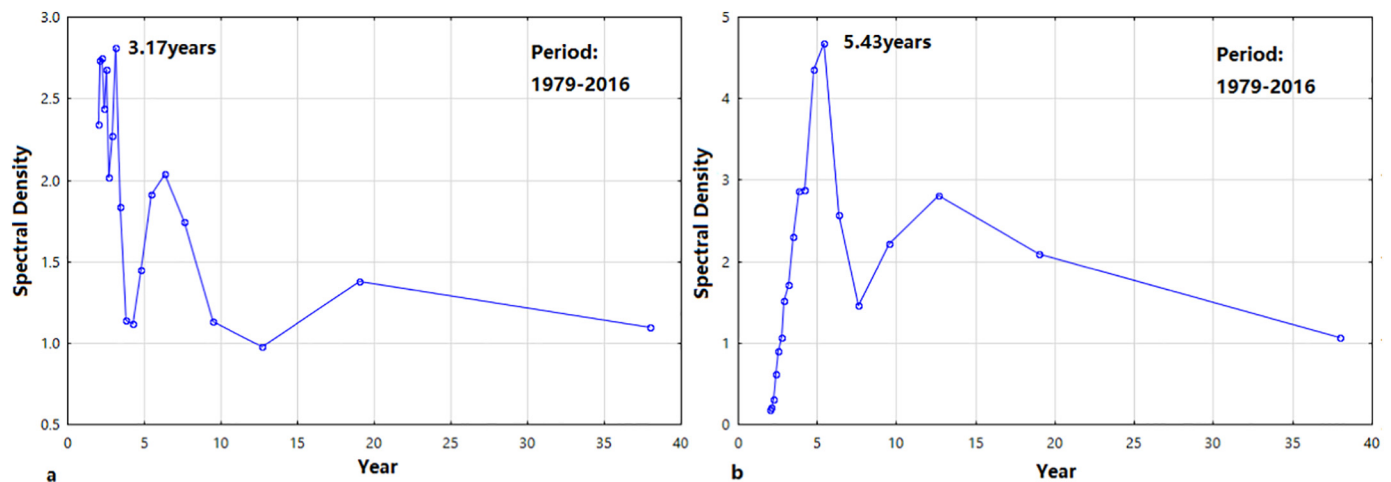


Fig. 7. Spectral analysis of the precipitation in coastal areas of eastern China (a) and the MEI (b). The main cycle is 3.17 years for the precipitation and 5.43 years for the MEI.

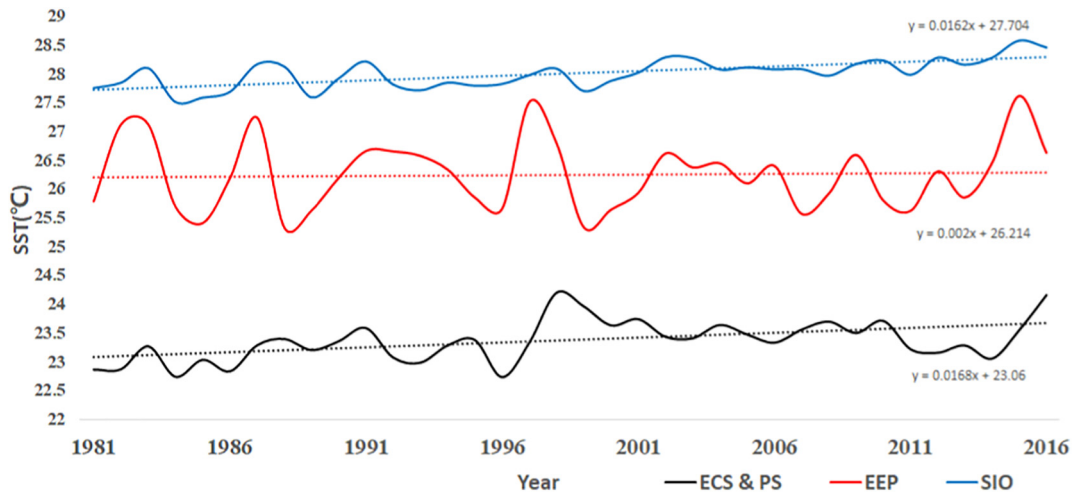


Fig. 8. The inter-annual variation of SST of three main correlated areas mentioned in fig. 1 (black: East China Sea (ECS) and the north of Philippine Sea (PS); red: Eastern Equatorial Pacific (EEP); and blue: subtropical Indian Ocean (SIO) from 1979 to 2016).

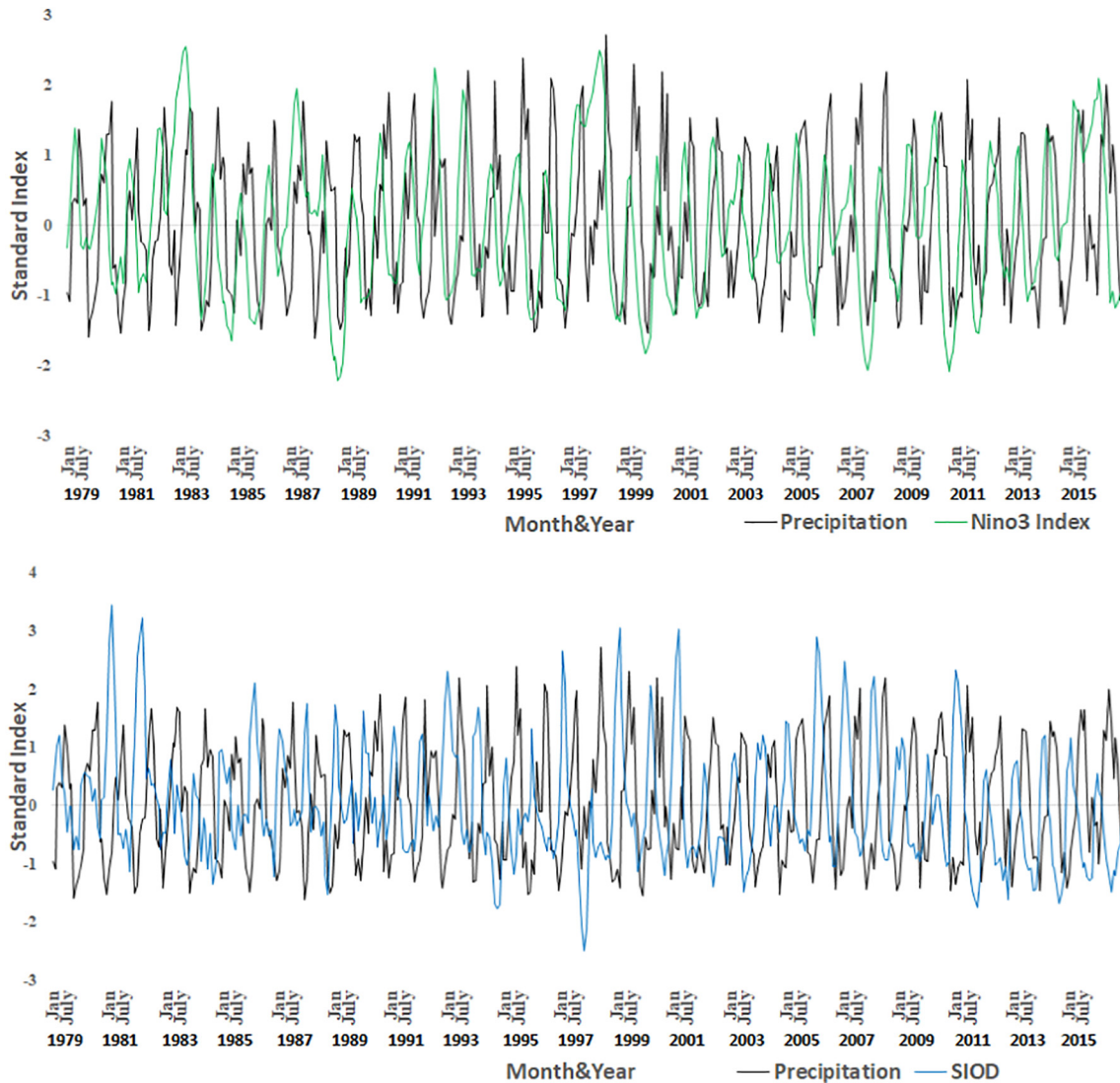


Fig. 9. Standard index of climate time-series and precipitation in coastal areas of eastern China (black: standard index of precipitation; green: standard index of Niño3 SST index; blue: standard index of SIOD index).

**Table 2**

The correlation coefficient between the antecedent precipitation and each subsequent climate time-series index (all values passed the significance test at the level of 95%).

Index lead month	Niño1 + 2	Niño3	SIOD
2	0.6096	0.6768	–
3	0.7835	0.6409	0.4526
4	–	–	0.5609

and north of the PS, the temperature increases from May to August, and drops from September to February. All of the four seasons' SSTs have been rising during the past 38 years there, of which the summer SST has the most significant upward trend. The results of the spectral analysis show that the time series of precipitation over the eastern China and the MEI have the similar cycles about 3 and 5 years, which can also indicate the correlation between the precipitation and the ENSO events.

We have shown that observed monthly mean rainfall and three SST indices are positively correlated, especially when the Niño 1 + 2 SST index leads precipitation by three months. Moreover, the Niño 3 and the SIOD index are also related to the previous precipitation.

### Author contributions

Chenxu Ji and Yuanzhi Zhang conceived and designed the experiments; Chenxu Ji and Qiuming Cheng performed the experiments and analyzed the data; Yu Li, Tingchen Jiang, and X. San Liang improved the data analysis; Chenxu Ji and Yuanzhi Zhang wrote the paper.

### Conflicts of interest

The authors declare no conflict of interest.

### Acknowledgments

The SST data and the local governmental data are highly appreciated. This research is jointly supported by the 'National Key Research and Development Program of China (Project Ref. No. 2016YFC1402003)', the State Key Lab Fund for Geological Processes and Mineral Resources (2016), and the '2015 Jiangsu Shuangchuang Program of China'.

### References

Behera, S.K., Yamagata, T., 2001. Subtropical SST dipole events in the southern Indian Ocean. *J. Geophys. Res. Lett.* 28, 327–330.

Cai, J., Zhang, Y., Li, Y., Liang, X.S., Jiang, T., 2017. Analyzing the characteristics of soil moisture using gldas data: A case study in eastern china. *Appl. Sci.* 7, 566.

Center, C.P., 2015. Historical el nino/la nina episodes (1950-present)[J]. In: National Oceanic Atmospheric Administration/National Weather Service [cited 24 May 2016], Available from: [http://www.cpc.noaa.gov/products/analysis\\_monitoring/ensostuff/ensoyears.shtml](http://www.cpc.noaa.gov/products/analysis_monitoring/ensostuff/ensoyears.shtml).

Chan, J.C.L., Zhou, W., 2005. PDO, ENSO and the early summer monsoon rainfall over south China[J]. *Geophys. Res. Lett.* 32(8).

Ding, Y., Wang, Z., Sun, Y., 2008. Inter-decadal variation of the summer precipitation in East China and its association with decreasing Asian summer monsoon. Part I: Observed evidences [J]. *Int. J. Climatol.* 28 (9), 1139–1161.

Ding, Y., Sun, Y., Wang, Z., et al., 2009. Inter-decadal variation of the summer precipitation in China and its association with decreasing Asian summer monsoon Part II: Possible causes[J]. *Int. J. Climatol.* 29 (13), 1926–1944.

Erwin, K., 1979. *Advanced Engineering Mathematics* (Fourth ed) [M]. Wiley, pp. 880 (eq. 5).

Feng, J., Li, J., 2011. Influence of El Niño Modoki on spring rainfall over south China[J]. *J. Geophys. Res. Atmos.* 116 (D13).

Ghil, M., Allen, M.R., Dettinger, M.D., et al., 2002. Advanced spectral methods for climatic time series[J]. *Rev. Geophys.* 40 (1), 3 -1-3-41.

Gong, S., Wong, K., 2018. Spatio-Temporal Analysis of Sea Surface Temperature in the East China Sea Using TERRA/MODIS Products Data[M]//Sea Level Rise and Coastal Infrastructure. IntechOpen.

Guan, Z., Yamagata, T., 2003. The unusual summer of 1994 in East Asia: IOD teleconnections[J]. *Geophys. Res. Lett.* 30(10).

Ji, C., Zhang, Y., Cheng, Q., Li, Y., Jiang, T., Liang, X.S., 2018a. On the relationship

between the early spring Indian ocean's sea surface temperature (SST) and the Tibetan plateau atmospheric heat source in summer. *Glob. Planet. Chang.* 164, 1–10.

Ji, C., Zhang, Y., Cheng, Q., Tsou, J.Y., Jiang, T., Liang, X.S., 2018b. Evaluating the impact of sea surface temperature (SST) on spatial distribution of chlorophyll-a concentration in the east china sea. *Int. J. Appl. Earth Obs. Geoinf.* 68, 252–261.

Kendall, G., 1975. *Rank Correlation Methods*, 4th ed. 1975, 4. Charles Griffin, London, UK, pp. 202.

Korn, F., Labrinidis, A., Kotidis, Y., et al., 1998. Ratio rules: A new paradigm for fast, quantifiable data mining[J].

Kumar, A., Chen, M., Wang, W., 2013. Understanding prediction skill of seasonal mean precipitation over the tropics[J]. *J. Clim.* 26 (15), 5674–5681.

Li, Y., Leung, L.R., 2013. Potential impacts of the Arctic on interannual and interdecadal summer precipitation over China[J]. *J. Clim.* 26 (3), 899–917.

Li, J., Wu, Z., Jiang, Z., et al., 2010a. Can global warming strengthen the East Asian summer monsoon?[J]. *J. Clim.* 23 (24), 6696–6705.

Li, H., Dai, A., Zhou, T., et al., 2010b. Responses of East Asian summer monsoon to historical SST and atmospheric forcing during 1950–2000[J]. *Clim. Dyn.* 34 (4), 501–514.

Liu, G., Wu, R., Zhang, Y., et al., 2014a. The summer snow cover anomaly over the Tibetan Plateau and its association with simultaneous precipitation over the mei-yu-baiu region[J]. *Adv. Atmos. Sci.* 31 (4), 755.

Liu, G., Wu, R.G., Zhang, Y.Z., 2014b. Persistence of snow cover anomalies over the Tibetan Plateau and the implications for forecasting summer precipitation over the Meiyu-Baiu Region[J]. *Atmos. Oceanic Sci. Lett.* 7 (2), 115–119.

Lu, R., Lu, S., 2014. Local and remote factors affecting the SST–precipitation relationship over the western North Pacific during summer[J]. *J. Clim.* 27 (13), 5132–5147.

Mann, B., 1945. Non-parametric tests against trend. *J. Econ.* 13, 163–171.

Mao-qiu, J., Hui-bang, L.U.O., Yun-ting, Q., 2004. On the relationships between the summer rainfall in China and the atmospheric heat sources over the eastern Tibetan Plateau and the western Pacific warm pool[J]. *J. Trop. Meteorol.* 10 (2), 133–143.

Ouyang, R., Liu, W., Fu, G., et al., 2014. Linkages between ENSO/PDO signals and precipitation, streamflow in China during the last 100 years[J]. *Hydrol. Earth Syst. Sci.* 18 (9), 3651–3661.

Pearson, K., 1895. Note on regression and inheritance in the case of two parents[J]. *Proc. R. Soc. Lond.* 58, 240–242.

Pelletier, J.D., 1998. The power spectral density of atmospheric temperature from time scales of 10– 2 to 106 yr[J]. *Earth Planet. Sci. Lett.* 158 (3-4), 157–164.

Privé, N.C., Plumb, R.A., 2007. Monsoon dynamics with interactive forcing. Part II: Impact of eddies and asymmetric geometries[J]. *J. Atmos. Sci.* 64 (5), 1431–1442.

Qiuming, Y., 2006. Indian Ocean subtropical dipole and variations of global circulations and rainfall in China[J]. *Acta Oceanol. Sin.* 28, 47–56.

Rasmusson, E.M., Wallace, J.M., 1983. Meteorological aspects of the El Niño/southern oscillation[J]. *Science* 222 (4629), 1195–1202.

Shukla, J., Paolino, D.A., 1983. The Southern Oscillation and long-range forecasting of the summer monsoon rainfall over India[J]. *Mon. Weather Rev.* 111 (9), 1830–1837.

Tao, S.Y., 1987. A review of recent research on the East Asian summer monsoon in China [J]. *Monsoon Meteorol.* 60–92.

Terray, P., Delécluse, P., Labattu, S., et al., 2003. Sea surface temperature associations with the late Indian summer monsoon[J]. *Clim. Dyn.* 21 (7-8), 593–618.

Tong, J., Qiang, Z., Deming, Z., et al., 2006. Yangtze floods and droughts (China) and teleconnections with ENSO activities (1470–2003) [J]. *Quat. Int.* 144 (1), 29–37.

Walker, G.T., 1925. Correlation in seasonal variations of weather—A further study of world weather[J]. *Mon. Weather Rev.* 53 (6), 252–254.

Wang, B., Wu, R., Fu, X., 2000. Pacific–East Asian teleconnection: how does ENSO affect East Asian climate? [J]. *J. Clim.* 13 (9), 1517–1536.

Wang, B., Ding, Q., Fu, X., et al., 2005. Fundamental challenge in simulation and prediction of summer monsoon rainfall[J]. *Geophys. Res. Lett.* 32(15).

Webster, P.J., Magana, V.O., Palmer, T.N., et al., 1998. Monsoons: Processes, predictability, and the prospects for prediction[J]. *J. Geophys. Res. Oceans* 103 (C7), 14451–14510.

Wu, R., Kirtman, B.P., 2007. Regimes of seasonal air–sea interaction and implications for performance of forced simulations[J]. *Clim. Dyn.* 29 (4), 393–410.

Wu, B., Zhou, T., Li, T., 2009. Contrast of rainfall–SST relationships in the western North Pacific between the ENSO-developing and ENSO-decaying summers[J]. *J. Clim.* 22 (16), 4398–4405.

Xiao, M., Zhang, Q., Singh, V.P., 2015. Influences of ENSO, NAO, IOD and PDO on seasonal precipitation regimes in the Yangtze River basin, China[J]. *Int. J. Climatol.* 35 (12), 3556–3567.

Xie, S.P., Hu, K., Hafner, J., et al., 2009. Indian Ocean capacitor effect on Indo-western Pacific climate during the summer following El Niño[J]. *J. Clim.* 22 (3), 730–747.

Xu, H., Zhang, L., Du, Y., 2013. Research progress of southern Indian Ocean dipole and its influence[J]. *J. Trop. Oceanogr.* 32 (1), 1–7.

Yang, F., Lau, K.M., 2004. Trend and variability of China precipitation in spring and summer: linkage to sea-surface temperatures[J]. *Int. J. Climatol.* 24 (13), 1625–1644.

Yu, R., Zhou, T., 2007. Seasonality and three-dimensional structure of interdecadal change in the East Asian monsoon[J]. *J. Clim.* 20 (21), 5344–5355.

Yuan, Y., Yang, H., Zhou, W., et al., 2008. Influences of the Indian Ocean dipole on the Asian summer monsoon in the following year[J]. *Int. J. Climatol.* 28 (14), 1849–1859.

Yue, S., Wang, C.Y., 2004. The Mann-Kendall test modified by effective sample size to detect trend in serially correlated hydrological series[J]. *Water Resour. Manag.* 18 (3), 201–218.

Zhang, Y., Ge, E., 2013. Temporal scaling behaviour of sea-level change in Hong Kong—Multifractal temporally weighted detrended fluctuation analysis. *Glob. Planet. Chang.* 100, 362–370.

Zhang, X., Alexander, L., Hegerl, G.C., et al., 2011. Indices for monitoring changes in

- extremes based on daily temperature and precipitation data[J]. *Wiley Interdisc. Rev.* 2 (6), 851–870.
- Zhang, L., Fraedrich, K., Zhu, X., et al., 2015. Interannual variability of winter precipitation in Southeast China[J]. *Theor. Appl. Climatol.* 119 (1-2), 229–238.
- Zhou, L.T., Wu, R., 2010. Respective impacts of the East Asian winter monsoon and ENSO on winter rainfall in China[J]. *J. Geophys. Res. Atmos.* 115 (D2).
- Zhou, L.T., Tam, C.Y., Zhou, W., et al., 2010. Influence of South China Sea SST and the ENSO on winter rainfall over South China[J]. *Adv. Atmos. Sci.* 27 (4), 832–844.
- Zhu, Y., Wang, H., Zhou, W., et al., 2011. Recent changes in the summer precipitation pattern in East China and the background circulation[J]. *Clim. Dyn.* 36 (7-8), 1463–1473.
- Zhu, Y., Liu, H., Ding, Y., et al., 2015. Interdecadal variation of spring snow depth over the Tibetan Plateau and its influence on summer rainfall over East China in the recent 30 years[J]. *Int. J. Climatol.* 35 (12), 3654–3660.